RSC Advances

PAPER

View Article Online
View Journal | View Issue

Cite this: *RSC Adv.*, 2020, **10**, 14007

Quasi-solid-state highly stretchable circular knitted MnO_2@CNT supercapacitor†

Taegyu Park, Yongwoo Jang, Jong Woo Park, Hyunsoo Kim and Seon Jeong Kim *

Flexible and stretchable fiber supercapacitors have been progressively improved for wearable electronic devices. However, they should be further improved with respect to stretchable range and stable electrochemical performance during dynamic movement when considering the tensile range for wearable applications. Here, we report a quasi-solid-state circular knitted MnO_2@CNT supercapacitor with high tensile range. To fabricate this, CNT fibers were knitted into a circular shape using a knitting machine then subsequently electrochemically deposited by a pseudocapacitive material, MnO_2. Consequently, the knitted MnO_2@CNT fiber supercapacitors were structurally 100% stretchable, and their energy storage performance remained stable during knitted capacitor stretching of up to 100%. Maximum linear capacitance and area capacitance are considerably large (321.08 mF cm^{-1}, 511.28 mF cm^{-2}). In addition, the supercapacitor showed negligible loss of capacitance after 10 000 repeated charge/discharge cycles and dynamic stretching cycle testing. Furthermore, we also provided double-walled knitted MnO_2@CNT supercapacitors by symmetrically inserting one knitted supercapacitor into another. The double-walled supercapacitor also exhibited a stable stretchability of up to 100% without loss of capacitance. Therefore, this highly stretchable fiber-type supercapacitor could be utilized for energy storage in wearable devices.

Received 13th February 2020
Accepted 27th March 2020

DOI: 10.1039/d0ra01398f

rsc.li/rsc-advances

Introduction

Construction of next-generation wearable technologies from textiles incorporating fiber-type sensors, energy harvesters, and supercapacitors has been attempted.[1–4] Flexible and stretchable supercapacitors have attracted great attention for application due to their enhanced movement in wearable devices. Hence, a number of supercapacitors have been proposed to increase movement and improve energy performance.[5–8] However, there are still limitations to supercapacitors with high performance over a wide tensile range.[2,3]

In wearable supercapacitors, increasing the flexibility and stretchability are the most important elements.[18–27] Therefore, many attempts have been conducted to improve the flexibility and stretchability in fiber-type supercapacitors. Initially, several studies showed flexible and stretchable supercapacitors produced by combining elastic polymers in the conductive electrodes.[3] These elastomer-based supercapacitors exhibit high tensile range, but electrical performances are significantly lower than those of other supercapacitors. As an alternative attempt, stable and improved flexibility and stretchability have been achieved by coiling the fiber-shaped supercapacitors, providing structural stretchability.[2–4] However, the structural stretchability is limited by tensile range. In fact, coiled supercapacitors are limited to a maximum of 50% of the tensile range.[12–16] Because the tensile range for wearable application requires a maximum of 100%, the tensile range of fiber-shaped supercapacitors should be improved.[5–8]

In the present study, a new supercapacitor structure with high tensile range and stable capacitance retention has been attempted. The knitted structures are built by interloping of yarns with anisotropic shape. Since the yarn loops can easily move across each other, the knitted structure is elastic and easy to shape. Hence, the knitted structure makes stretchability with high tensile range possible. In addition, the knitted structure would exhibit no change in capacitance during the tensile changes induced by structural movement. Therefore, this knitted structure offers great advantages in achieving high flexibility and stretchability of the supercapacitor.

Here, we report a stretchable double-walled supercapacitor with circular knitted structure. The electrodes with circular knitted structure were fabricated by a knitting machine with carbon nanotube fibers that have high conductivity in order to exhibit excellent capacitance and sufficient mechanical strength to withstand the torsional stress during the knitting process.[10,11] To improve intrinsic capacitance, the knitted CNT

Center for Self-powered Actuation, Department of Biomedical Engineering, Hanyang University, Seoul 04736, Korea. E-mail: sjk@hanyang.ac.kr

† Electronic supplementary information (ESI) available. See DOI: 10.1039/d0ra01398f

electrodes were electrochemically deposited by using a transition metal oxide, MnO_2, as a pseudocapacitive material.[17] The application of MnO_2 in supercapacitors is highly attractive due to high capacitance, environmental compatibility, natural abundance, and low cost.[9] Two cylindrical MnO_2@CNT electrodes were symmetrically overlapped in the form of a single body, similar to the double-wall structure, and then a PVA/LiCl gel electrolyte was coated between the electrodes.[28–31] Consequently, the double-walled MnO_2@CNT supercapacitor was able to stretch to 100% structurally, and its maximum linear and areal capacitance values are 321.08 mF cm^{-1} and 511.28 mF cm^{-2}. Areal energy density and power density are, respectively, 45.44 μW h cm^{-2} and 648 μW cm^{-2}, higher values than those of other stretchable supercapacitors. Moreover, the supercapacitor showed negligible capacitance loss after 500 repeated stretching cycles.

Results and discussion

Fabrication of a knitted double-wall MnO_2@CNT supercapacitor

A knitted double-wall MnO_2@CNT supercapacitor is illustrated in Fig. 1a. As an electrode, CNT yarns were knitted into circular shape by using a knitting machine. Thereafter, the knitted CNT electrodes were electrochemically deposited by using a transition metal oxide, MnO_2, as a pseudocapacitive material. The knitted MnO_2@CNT supercapacitor is cylindrical, and this structure enables combination of two electrodes. Therefore, the electrodes were symmetrically combined and then coated using PVA/LiCl gel electrolyte. Finally, silicone was coated on the gel electrolyte to prevent the gel electrolyte from escaping. Electrochemical deposition was performed during 20 minutes in the condition of 0.03 M manganese(II) acetate tetrahydrate and 0.1 M lithium chloride solution using the potentiometric method. The loading level of guest MnO_2 was controlled by deposition time. Longer deposition time resulted in higher capacitance values due to higher loadings, but it showed a reduced capacitance retention (Fig. S5†). The MnO_2 loading level of MnO_2-coated knitted CNT fiber is 84.6 wt% through electro-deposition. Fig. 1b shows the stretching of the knitted structure. The knitted structure makes it possible to structurally increase and decrease the length. This stretching motion is altered by a change in the shape of the inner ring; thus, no physical change of the fiber occurs with the change in length. Thus, the knit structure is structurally movable, and so there is no need to combine other elastomers with the electrodes. Fig. 1c is a scanning electron microscope (SEM) image showing deposited MnO_2 on yarn loops of knitted CNT yarns. The figure shows that manganese is deposited evenly across the rings. In Fig. S4,† the cross-section SEM image of MnO_2@CNT fiber shows the deposition in the form of a core–shell. Furthermore, the MnO_2 was characterized by Energy Dispersive X-ray Spectroscopy and EDS mapping (Fig. 1d and S1†). The EDS analysis in Fig. S1† shows that the atomic ratios of C, O, and Mn are 38.63%, 42.54%, and 14.93%, respectively, indicating that manganese is deposited on the CNT fibers. Elemental mapping analysis for C, O, and Mn atoms was performed on the Fig. 1d image to detect the locations of specific atoms within the knitted MnO_2@CNT fiber. Fig. 1d shows that the green, yellow, and red dots represent C, O, and Mn atoms, respectively, and that the atoms of Mn and O are evenly distributed on the CNT fiber.

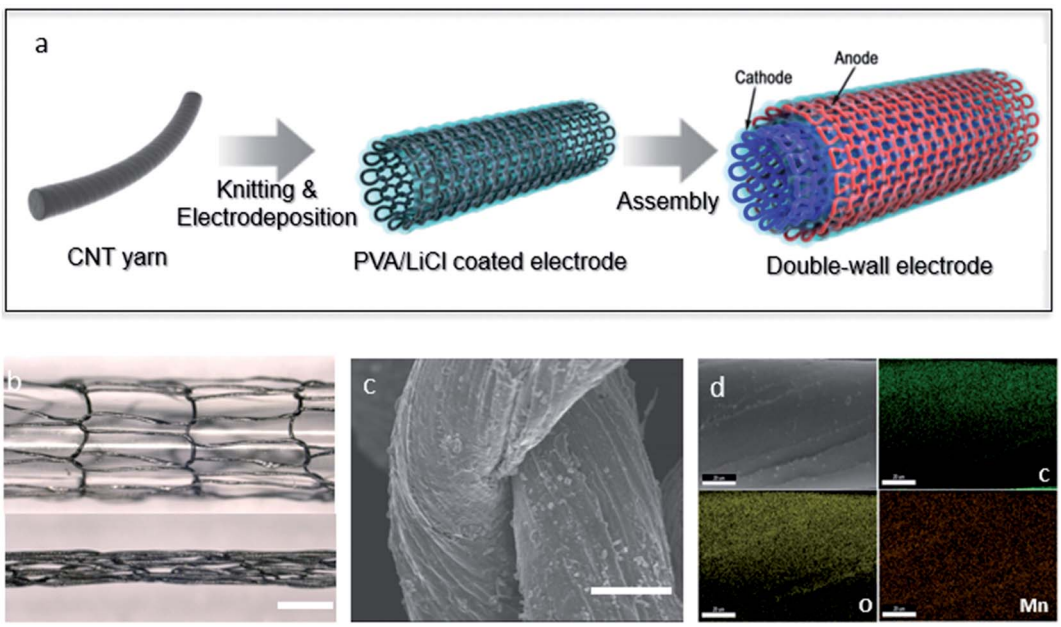

Fig. 1 Fabrication scheme and images of a knitted MnO_2@CNT fiber supercapacitor. (a) Schematic illustration of a double-wall structure of knitted MnO_2@CNT fiber supercapacitor. (b) Optical image of non-stretched ($\varepsilon = 0$) and stretching ($\varepsilon = 100\%$) state knitted structure (scale bar: 1 mm). (c) SEM image of a knitted MnO_2@CNT fiber (scale bar, 500 μm & 50 μm). (d) EDX mapping images of knitted MnO_2@CNT fiber supercapacitor (scale bar: 20 μm).

Electrochemical performance of a knitted MnO_2@CNT supercapacitor

The electrochemical performance of a knitted double-wall MnO_2@CNT electrode is shown in Fig. 2. Measurement of cyclic voltammetry (CV) showed the rectangular dependence of current density on applied potential, which was retained for scan rates up to 100 V s^{-1}, and CV graphs at different scan rates are shown in Fig. 1a. The rectangular CV curves without any faradaic redox peaks are consistent with the energy storage process using a combination of the electrochemical double-layer capacitance (EDLC) of the CNTs and the pseudo-capacitance of MnO_2. Galvanic charge/discharge curves for the capacitors exhibited triangular charge/discharge patterns that are consistent with energy storage by electrochemical double-layer charging capacitance of the CNT and the pseudo-capacitance of MnO_2 (Fig. 2b). Fig. 2c shows areal and linear capacitance as a function of scan rate from 10 mV s^{-1} to 100 mV s^{-1} for the knitted MnO_2@CNT supercapacitor. The highest values of the area and linear-normalized specific capacitances from the CV graph are 511.28 mF cm^{-2} and 321.08 mF cm^{-1}, respectively, at a voltage scan rate of 10 mV s^{-1}. The normalized value for the area is a value with significant loss, as a characteristic of the knit structure. This is because the knit structure contains many holes on the surface, and the normalized value for the area also includes the area of these holes. Likewise, normalization for volume is not accurate because the interior is empty. The knitted MnO_2@CNT supercapacitor exhibited negligible loss in capacity after 10 000 repeated charge/discharge cycles, indicating the stability of capacitance retention for 10 000 cycles (Fig. 2d).[32–34]

Electrochemical impedance spectroscopy measurement is shown in Fig. 2e. A vertical line of the Nyquist curve indicates an excellent capacitive characteristic of the knitted MnO_2@CNT supercapacitor. The initial equivalent series resistance (ESR) of the Nyquist curve was 54 Ω cm^{-1}, which is lower than that of the CNT yarn with the same weight. Resistance increases as the fiber lengthens, but resistance decreases due to contact within the fiber when the same weight of fiber forms a knit structure. The inset shows the equivalent circuit. The real axial section at high frequencies corresponds to electrolyte resistance (R_s) and is also called equivalent series resistance (ESR). C_{dl} is a constant phase element (CPE) that exhibits double layer capacitance occurring at the interface between a solid and an ionic solution due to separation of ionic or electron charges. W is the Warburg factor representing the diffusion of ions from the intermediate frequency domain to the porous electrode. As shown in Fig. 2f, negligible changes were observed in the resistance curves of the knitted MnO_2@CNT supercapacitor when strains of 20, 40, 60, 80, and 100% were applied. Taken together, these results indicate that the energy storage performance remains stable during knitted capacitor stretching up to 100%.

Stretchability of a one-body double-wall knitted MnO_2@CNT fiber supercapacitor

Furthermore, we attempted to symmetrically combine two knitted MnO_2@CNT supercapacitors, inserting one knitted supercapacitor into another. Since the cylindrical knit structure is hollow inside, it is possible to combine two electrodes into one. The PVA/LiCl gel electrolyte is then coated onto the fabricated one-body electrode. The coated gel electrolyte was also able to

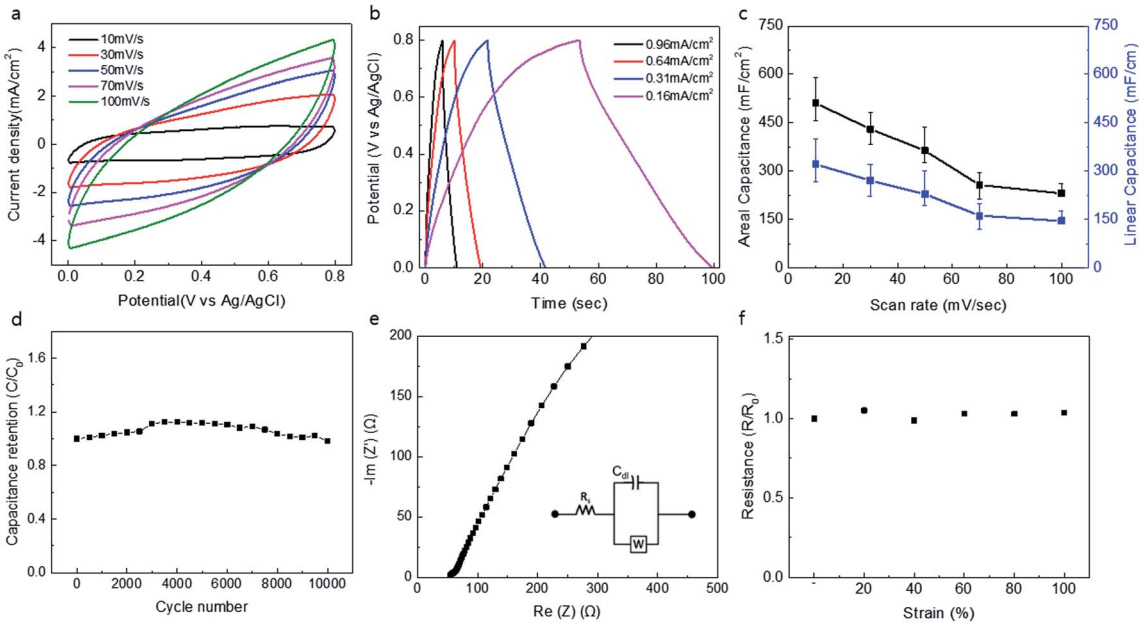

Fig. 2 Electrochemical performance of a knitted MnO_2@CNT fiber supercapacitor (a) CV curves measured from 10 to 100 mV s^{-1} for knitted MnO_2@CNT fiber. (b) Galvanostatic charge/discharge curves measured from 0.16 mA cm^{-2} to 0.96 mA cm^{-2} current densities. (c) Linear capacitance and areal specific capacitance of knitted MnO_2@CNT fiber. (d) Capacitance retention of supercapacitor during 10 000 charge/discharge cycles. (e) Nyquist curve for the frequency range from 0.01 to 1 kHz. Inset: equivalent circuit. (f) Resistance of knitted MnO_2@CNT fiber supercapacitor in various stretching ranges (0–100%).

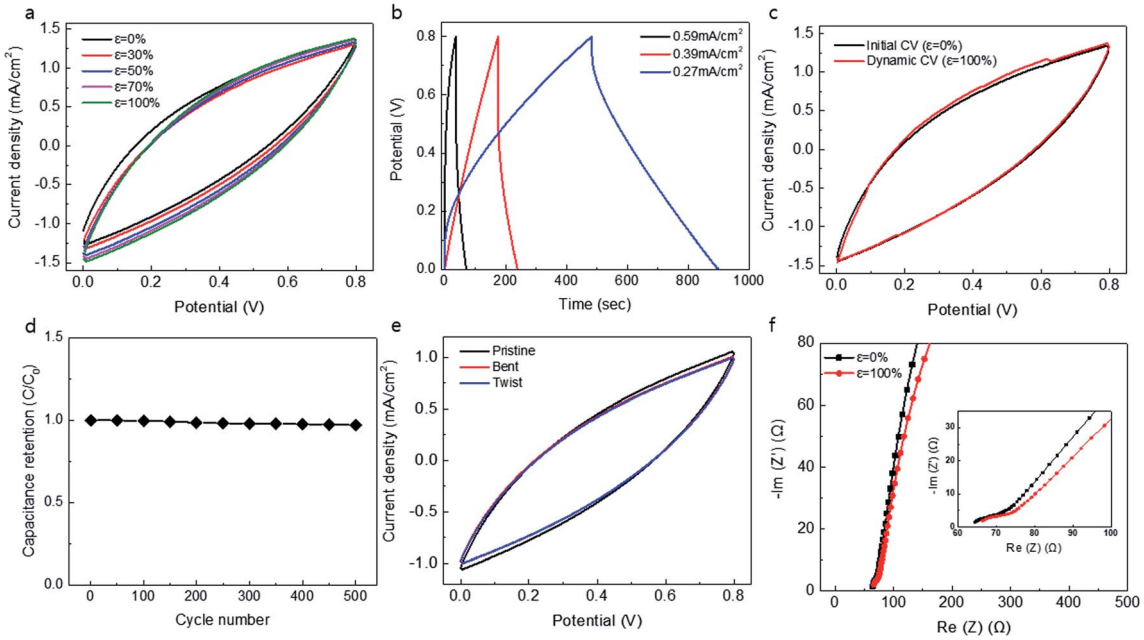

Fig. 3 Stretchability of a double-wall knitted MnO_2@CNT fiber supercapacitor (a) CV curves (at 10 mV s^{-1}) measured for the initial ($\varepsilon = 0\%$) and statically stretched states ($\varepsilon = 30, 50, 70, 100\%$) of the stretchable supercapacitors made from knitted MnO_2/CNT fiber coated with PVA/LiCl gel electrolyte. (b) Galvanostatic charge/discharge (GCD) curves measured for symmetric one-body knitted MnO_2/CNT fiber supercapacitor from 0.27 mA cm^{-2} to 0.59 mA cm^{-2} current densities. (c) Dynamically measured CV curves (at 10 mV s^{-1} scan rate) during 100% strain stretching/releasing cycles. Non-stretched ($\varepsilon = 0$) a double-wall knitted supercapacitor CV curves are denoted for comparison (black line), while dynamically measured CV curves with stretching ($\varepsilon = 100\%$) state (red line). (d) Capacitance retention measured for the initial ($\varepsilon = 0\%$) and statically stretched states ($\varepsilon = 100\%$) of a double-wall knitted CNT/MnO_2 supercapacitor during repeat straining cycles. (e) CV curves (at 50 mV s^{-1}) for non-deformed, bent, twisted one-body knitted MnO_2/CNT fiber supercapacitor. (f) Nyquist curves measured for initial ($\varepsilon = 0\%$) and statically stretched states ($\varepsilon = 100\%$) of a double-wall knitted CNT/MnO_2 supercapacitor.

prevent shorting between two knitted supercapacitors. Fig. 3 shows the electrochemical performance and the stretchability of a one-body double-wall knitted MnO_2@CNT fiber supercapacitor. Fig. 3a shows the CV graph for the stretching length of a one-body double-wall knitted supercapacitor. Despite the overlap of the two knitted supercapacitors, it exhibits stable stretchability up to 100% without change of capacitance. Fig. 3b shows a galvanostatic charge/discharge curves of the performance in a PVA gel electrolyte with a symmetrical knit structure. Fig. 3c shows dynamically measured CV curves (at 10 mV s^{-1} scan rate) during 100% strain stretching/releasing cycles. It exhibits 98% capacitance retention during dynamic stretching. It is demonstrated that dynamically applied cyclic strains during capacitor charge and discharge do not degrade supercapacitor performance. Fig. 3d shows the stability of the supercapacitor during repeated stretching cycles. The figure exhibits a negligible change in capacitance over 500 cycles. To evaluate flexibility, the double-wall knitted supercapacitor was bent to a maximum 160° and twisted at approximately 2.27 rad cm^{-1} (Fig. 3e). The double-wall knitted supercapacitor was completely unaffected by dynamic application of twisting and bending. As shown in the Nyquist curves of Fig. 3f, negligible changes in the initial equivalent series resistance of the knitted MnO_2@CNT supercapacitor were observed compared to when 0 and 100% strains were applied. Overall, the double-wall knitted MnO_2@CNT supercapacitor exhibited a remarkably stable electrochemical performance during dynamic cycles of 100% stretching. It is likely that its stability is attributed to structural movement without change in total length of the knitted structure when stretched.

Conclusion

In summary, the present study presented a double-wall knitted MnO_2@CNT supercapacitor that exhibits high electrochemical stability and excellent structural stretchability without the need for elastic polymers. In addition to high stretchability of up to 100%, a knitted MnO_2@CNT supercapacitor showed high areal capacitance (511.28 mF cm^{-2}) and linear capacitance (321.08 mF cm^{-1}). This performance is superior to those of other stretchable supercapacitors with elastomers. The supercapacitor is easy to fabricate and scale up for applications in electronic textiles because current supercapacitors can be simply knitted by knitting machines. Furthermore, quasi-solid-state MnO_2@CNT supercapacitors can be sewn as a single thread into textiles to power small electronic devices.

Experimental section

Preparation of knitted MnO_2@CNT fiber electrode

Commercial CNT fiber (C-type, 55 mm diameter and 40° twist) from Muratec (JP) was used as a current collector. The knitted CNT fiber was fabricated by a knitting machine (ST2B/HS-R)

from LAMB Knitting Machine Corporation (USA). After knitting the commercial CNT fiber, the knitted CNT fiber was 2 mm in diameter. The electrochemical deposition was performed using 0.03 M manganese(II) acetate tetrahydrate and 0.1 M lithium chloride solution. All materials were purchased from Sigma-Aldrich (USA). Electrochemical deposition of MnO_2 onto the knitted CNT fiber electrode was performed using a potentiostatic method. Approximately 1.3 V (*vs.* Ag/AgCl as a reference electrode and Pt mesh as a counter electrode in a three-electrode system) was applied for 20 minutes using an electrochemical analyzer (CHI 627b system, CH Instruments, Austin, TX).

One-body supercapacitor assembly

The PVA/LiCl gel electrolyte was prepared by heating a mixture of 3 g PVA (M_w 146 000–186 000) and 6 g LiCl in 30 mL deionized water at 90 °C for several hours. First, one knitted electrode was coated with PVA/LiCl gel electrolyte to assemble a one-body supercapacitor. The other knitted electrode was combined, and the gel electrolyte was coated onto the electrodes. After that, silicone was coated on and dried. All chemicals for electrolyte synthesis were purchased from Sigma-Aldrich (USA).

Characterization

Electrochemical measurements of the knitted MnO_2@CNT fiber supercapacitor utilized an electrochemical analyzer (CHI 627b, CH Instruments). Dynamic measurements of CV curves were made on a fiber supercapacitor by cycling at 50 mV s^{-1}, while the supercapacitor was stretched and released at set strain rates of 6.25% per second by using a specially constructed machine for applying tensile deformations. SEM images were obtained by using a Hitachi SEM-S4700 microscope. The length of the supercapacitor was measured using a digital Vernier caliper (500 Series, Mitutoyo), which was incorporated into the stretching machine. Stress–strain curves were obtained by using a mechanical analyzer (Shimadzu model: EZ-SX, Japan).

Specific capacitance calculation

The capacitance of the knitted MnO_2@CNT fiber supercapacitor was calculated from the CV curves. From $C = I/(dV/dt)$, I is average current and dV/dt is the voltage scan rate. The specific areal capacitance for each electrode in a supercapacitor having equal anode and cathode capacitances was calculated using $C_A = 4C/A$, where A is the total surface area of the anode and cathode. Additionally, the specific volumetric capacitance for each electrode in a supercapacitor having equal anode and cathode capacitances was calculated using $C_v = 4C/V$, where V is the total volume of the anode and cathode. For a given constant scan rate v and initial discharge voltage (V_i), the average power was calculated by integrating the current (I) *versus* voltage (V) curves;

$$P_{av} = V_i^{-1} \int_{V_1}^{0} IV\,dV$$

The energy was calculated by using equation;

$$E = \frac{1}{3600v} \int_{V_1}^{0} IV\,dV$$

Conflicts of interest

There are no conflicts to declare.

Acknowledgements

This work was supported by the Creative Research Initiative Center for Self-powered Actuation in the National Research Foundation of Korea.

References

1 J. A. Lee, M. K. Shin, S. H. Kim, H. U. Cho, G. M. Spinks, G. G. Wallace, M. E. Kozlov, R. H. Baughman, S. J. Kim, D. Lima and X. Lepro, *Nat. Commun.*, 2013, **4**, 1–8.
2 C. Choi, J. A. Lee, A. Y. Choi, Y. T. Kim, X. Lepro, M. D. Lima, R. H. Baughman and S. J. Kim, *Adv. Mater.*, 2014, **26**, 2059–2065.
3 C. Choi, S. H. Kim, H. J. Sim, J. A. Lee, A. Y. Choi, Y. T. Kim, X. Lepro, G. M. Spinks, R. H. Baughman and S. J. Kim, *Sci. Rep.*, 2015, **5**, 1–6.
4 C. Choi, H. J. Sim, G. M. Spinks, X. Lepro, R. H. Baughman and S. J. Kim, *Adv. Energy Mater.*, 2016, **6**, 1–8.
5 J. D. W. Madden, N. A. Vandesteeg, P. A. Anquetil, P. G. A. Madden, A. Takshi, R. Z. Pytel, S. R. Lafontaine, P. A. Wieringa and I. W. Hunter, *IEEE J. Oceanic Eng.*, 2004, **29**, 706–728.
6 P. Brochu and Q. Pei, *Macromol. Rapid Commun.*, 2010, **31**, 10–36.
7 R. Pelrine, R. Kornbluh, J. Joseph, R. Heydt, Q. Pei and S. Chiba, *Science*, 2000, **287**(5454), 836–839.
8 R. D. Kornbluh, R. Pelrine, Q. Pei, R. Heydt, S. Stanford, S. Oh and J. Eckerle, *Smart Struct. Mater. 2002 Ind. Commer. Appl. Smart Struct. Technol.*, 2002, vol. 4698, pp. 254–270.
9 G. Yu, L. Hu, M. Vosgueritchian, H. Wang, X. Xie, J. R. McDonough, X. Cui, Y. Cui and Z. Bao, *Nano Lett.*, 2011, **11**, 2905–2911.
10 J. Ren, L. Li, C. Chen, X. Chen, Z. Cai, L. Qiu, Y. Wang, X. Zhu and H. Peng, *Adv. Mater.*, 2013, **25**, 1155–1159.
11 X. Chen, L. Qiu, J. Ren, G. Guan, H. Lin, Z. Zhang, P. Chen, Y. Wang and H. Peng, *Adv. Mater.*, 2013, **25**, 6436–6441.
12 L. Kou, T. Huang, B. Zheng, Y. Han, X. Zhao, K. Gopalsamy, H. Sun and C. Gao, *Nat. Commun.*, 2014, **5**, 1–10.
13 D. Yu, K. Goh, H. Wang, L. Wei, W. Jiang, Q. Zhang, L. Dai and Y. Chen, *Nat. Nanotechnol.*, 2014, **9**, 555–562.
14 C. S. Haines, M. D. Lima, N. Li, G. M. Spinks, J. Foroughi, J. D. W. Madden, S. H. Kim, S. Fang, M. J. De Andrade, F. Goktepe, O. Goktepe, S. M. Mirvakili, S. Naficy, X. Lepro, J. Oh, M. E. Kozlov, S. J. Kim, X. Xu, B. J. Swedlove, G. G. Wallace and R. H. Baughman, *Sci. 80*, 2014, **343**, 868–872.

15 M. Zhang, K. R. Atkinson and R. H. Baughman, *Sci. 80*, 2004, **306**, 1358–1361.
16 M. D. Lima, N. Li, M. Jung de Andrade, S. Fang, J. Oh, G. M. Spinks, M. E. Kozlov, C. S. Haines, D. Suh, J. Foroughi, S. J. Kim, Y. Chen, T. Ware, M. K. Shin, L. D. Machado, A. F. Fonseca, J. D. W. Madden, W. E. Voit, D. S. Galvao, R. H. Baughman and R. H. Baughman, *Sci. 80*, 2012, **338**, 928–932.
17 C. Choi, K. M. Kim, K. J. Kim, X. Lepro, G. M. Spinks, R. H. Baughman and S. J. Kim, *Nat. Commun.*, 2016, **7**, 1–8.
18 J. Ren, L. Li, C. Chen, X. Chen, Z. Cai, L. Qiu, Y. Wang, X. Zhu and H. Peng, *Adv. Mater.*, 2013, **25**, 1155–1159.
19 D. Yu, K. Goh, Q. Zhang, L. Wei, H. Wang, W. Jiang and Y. Chen, *Adv. Mater.*, 2014, **26**, 6790–6797.
20 P. Xu, B. Wei, Z. Cao, J. Zheng, K. Gong, F. Li, J. Yu, Q. Li, W. Lu, J. H. Byun, B. S. Kim, Y. Yan and T. W. Chou, *ACS Nano*, 2015, **9**, 6088–6096.
21 J. Bae, M. K. Song, Y. J. Park, J. M. Kim, M. Liu and Z. L. Wang, *Angew. Chem., Int. Ed.*, 2011, **50**, 1683–1687.
22 Y. Meng, Y. Zhao, C. Hu, H. Cheng, Y. Hu, Z. Zhang, G. Shi and L. Qu, *Adv. Mater.*, 2013, **25**, 2326–2331.
23 K. Wang, Q. Meng, Y. Zhang, Z. Wei and M. Miao, *Adv. Mater.*, 2013, **25**, 1494–1498.
24 B. Wang, X. Fang, H. Sun, S. He, J. Ren, Y. Zhang and H. Peng, *Adv. Mater.*, 2015, 7854–7860.
25 V. T. Le, H. Kim, A. Ghosh, J. Kim, J. Chang, Q. A. Vu, D. T. Pham, J. H. Lee, S. W. Kim and Y. H. Lee, *ACS Nano*, 2013, **7**, 5940–5947.
26 Q. Meng, K. Wang, W. Guo, J. Fang, Z. Wei and X. She, *Small*, 2014, **10**, 3187–3193.
27 Z. Zhang, J. Deng, X. Li, Z. Yang, S. He, X. Chen, G. Guan, J. Ren and H. Peng, *Adv. Mater.*, 2015, **27**, 356–362.
28 Z. Pan, Y. Qiu, J. Yang, F. Ye, Y. Xu, X. Zhang, M. Liu and Y. Zhang, *Nano Energy*, 2016, **26**, 610–619.
29 T. Purkait, G. Singh, D. Kumar, M. Singh and R. S. Dey, *Sci. Rep.*, 2018, **8**(1), 1–13.
30 T. Chen, Y. Tang, Y. Qiao, Z. Liu, W. Guo, J. Song, S. Mu, S. Yu, Y. Zhao and F. Gao, *Sci. Rep.*, 2016, **6**, 23289.
31 J. Yu, W. Lu, J. P. Smith, K. S. Booksh, L. Meng, Y. Huang, Q. Li, J. Byun, Y. Oh, Y. Yan and T. W. Chou, *Adv. Energy Mater.*, 2017, **7**(3), 1600976.
32 T. Zhai, S. Sun, X. Liu, C. Liang, G. Wang and H. Xia, *Adv. Mater.*, 2018, **30**(12), 1706640.
33 T. Xiong, T. L. Tan, L. Lu, W. S. V. Lee and J. Xue, *Adv. Energy Mater.*, 2018, **8**(14), 1702630.
34 W. Xu, Z. Jiang, Q. Yang, W. Huo, M. S. Javed, Y. Li and C. Hu, *Nano Energy*, 2018, **43**, 168–176.

